Deletion of the proton receptor OGR1 in mouse osteoclasts impairs metabolic acidosis-induced bone resorption

see commentary on page 542

Nancy S. Krieger[1], Luojing Chen[1], Jennifer Becker[1], Michaela R. Chan[1] and David A. Bushinsky[1]

[1]Division of Nephrology, Department of Medicine, University of Rochester School of Medicine, Rochester, New York, USA

Metabolic acidosis induces osteoclastic bone resorption and inhibits osteoblastic bone formation. Previously we found that mice with a global deletion of the proton receptor OGR1 had increased bone density although both osteoblast and osteoclast activity were increased. To test whether direct effects on osteoclast OGR1 are critical for metabolic acidosis stimulated bone resorption, we generated knockout mice with an osteoclast-specific deletion of OGR1 (knockout mice). We studied bones from three-month old female mice and the differentiated osteoclasts derived from bone marrow of femurs from these knockout and wild type mice. MicroCT demonstrated increased density in tibiae and femurs but not in vertebrae of the knockout mice. Tartrate resistant acid phosphatase staining of tibia indicated a decrease in osteoclast number and surface area/bone surface from knockout compared to wild type mice. Osteoclasts derived from the marrow of knockout mice demonstrated decreased pit formation, osteoclast staining and osteoclast-specific gene expression compared to those from wild type mice. In response to metabolic acidosis, osteoclasts from knockout mice had decreased nuclear translocation of NFATc1, a transcriptional regulator of differentiation, and no increase in size or number compared to osteoclasts from wild type mice. Thus, loss of osteoclast OGR1 decreased both basal and metabolic acidosis-induced osteoclast activity indicating osteoclast OGR1 is important in mediating metabolic acidosis-induced bone resorption. Understanding the role of OGR1 in metabolic acidosis-induced bone resorption will provide insight into bone loss in acidotic patients with chronic kidney disease.

Kidney International (2021) **99,** 609–619; https://doi.org/10.1016/j.kint.2020.10.023

KEYWORDS: metabolic acidosis; OGR1; osteoclast

Correspondence: *Nancy S. Krieger, Division of Nephrology, Department of Medicine, University of Rochester School of Medicine, Box 675, 601 Elmwood Ave., Rochester, New York 14642, USA. E-mail: Nancy_Krieger@urmc.rochester.edu*

Received 29 April 2020; revised 30 September 2020; accepted 9 October 2020; published online 4 November 2020

Translational Statement

During chronic metabolic acidosis, bone calcium is lost while buffering systemic acidity. Using a mouse model, we found that acidosis decreases osteoblastic mineralization and stimulates osteoclastic bone resorption and that the osteoblastic proton receptor ovarian cancer G protein–coupled receptor 1 mediates this response. The present study addresses whether there is also a direct effect of acidosis on osteoclasts by selectively deleting osteoclastic ovarian cancer G protein–coupled receptor 1. We demonstrate that deletion of osteoclastic ovarian cancer G protein–coupled receptor 1 directly inhibits metabolic acidosis–induced bone resorption indicating the importance of this osteoclastic receptor. Characterization of the role of ovarian cancer G protein–coupled receptor 1 in metabolic acidosis–induced bone resorption will help understand and perhaps treat the bone loss in patients with acidosis and chronic kidney disease.

During chronic metabolic acidosis (MET), there is loss of calcium (Ca) from bone mineral in the process of buffering systemic acidity.[1] On the basis of the results from an *in vitro* physiological model of MET, we found an initial loss of Ca from bone initially through physicochemical mineral dissolution, with enhanced cell-mediated bone resorption by 24 hours.[2–6] MET decreases osteoblastic collagen synthesis and mineralization and stimulates osteoclastic bone resorption.[2] MET-induced bone resorption is mediated by an initial increase in intracellular Ca signaling[7–9] and stimulation of osteoblastic cyclooxygenase 2,[10,11] leading to a prostaglandin E_2–mediated increase in the receptor activator of nuclear factor κB ligand (RANKL) expression.[12,13] RANKL interacts with its receptor on osteoclast (OC) precursors and promotes differentiation and activation of OCs and increased bone resorption.[14,15] Most recently, we have found that MET also stimulates the production of fibroblast growth factor 23 by these same mechanisms in the osteoblast.[16,17]

Ovarian cancer G protein–coupled receptor 1 (OGR1 or GPR68) is a proton-sensing receptor and is found in many tissues,[18,19] including bone.[20] OGR1 expression is highly upregulated in many cancers and may play a role in tumor biology[18] and is important in the response of bone to acidosis.[7,20–22] We found that MET increases intracellular Ca

in primary neonatal mouse calvarial osteoblasts through activation of OGR1,[7] suggesting that it is an osteoblast proton sensor. To characterize the role of OGR1 in the response of bone to MET, we studied bone from rapidly growing mice with a global deletion of OGR1 (OGR1−/−). There were no gross phenotypic differences between OGR1−/− and wild-type (WT) mice, but there was an increase in bone mineral density (BMD) in knockout mice compared with WT mice.[22] OGR1−/− bones had increased osteoblast numbers, an increase in bone formation rate, and osteoblastic gene expression. However, we also found an increase in OC number and surface area histochemically; isolated OC activity was not studied. These findings indicate that in rapidly growing mice, which generate large amounts of metabolic acid, the global lack of the proton receptor OGR1 leads to an increase in osteoblastic bone formation, which must be greater than any increase in OC activity. Others have shown that OGR1 is also present in the OC and may have a role in OC function and survival.[23–26] In the present study, we tested the hypothesis that direct effects on OGR1 in the OC are critical for MET stimulation of bone resorption by generating conditional knockout mice with an OC-specific deletion of OGR1 (osteoclastic conditional knockout [OC-cKO]).

RESULTS

OC-specific deletion of OGR1

We successfully bred OGR1-floxed (fl/fl) mice (WT for all experiments) with LysM-Cre mice to generate OC-cKO mice. There were no gross phenotypic differences between OGR1 fl/fl mice and OC-cKO mice. After genotyping the mice, bone marrow or spleen cells from 3-month-old homozygous WT or OC-cKO were cultured under conditions leading to differentiated OCs and which were used to verify *Ogr1* deletion specifically in OCs. A deletion of *Ogr1* in homozygote OC-cKO cells, but not in WT cells, was identified by specific polymerase chain reaction (PCR) (Figure 1a). In Supplementary Figure S1, we show that this deletion is not present in osteoblasts from OC-cKO mice, supporting the specificity of OC knockout of

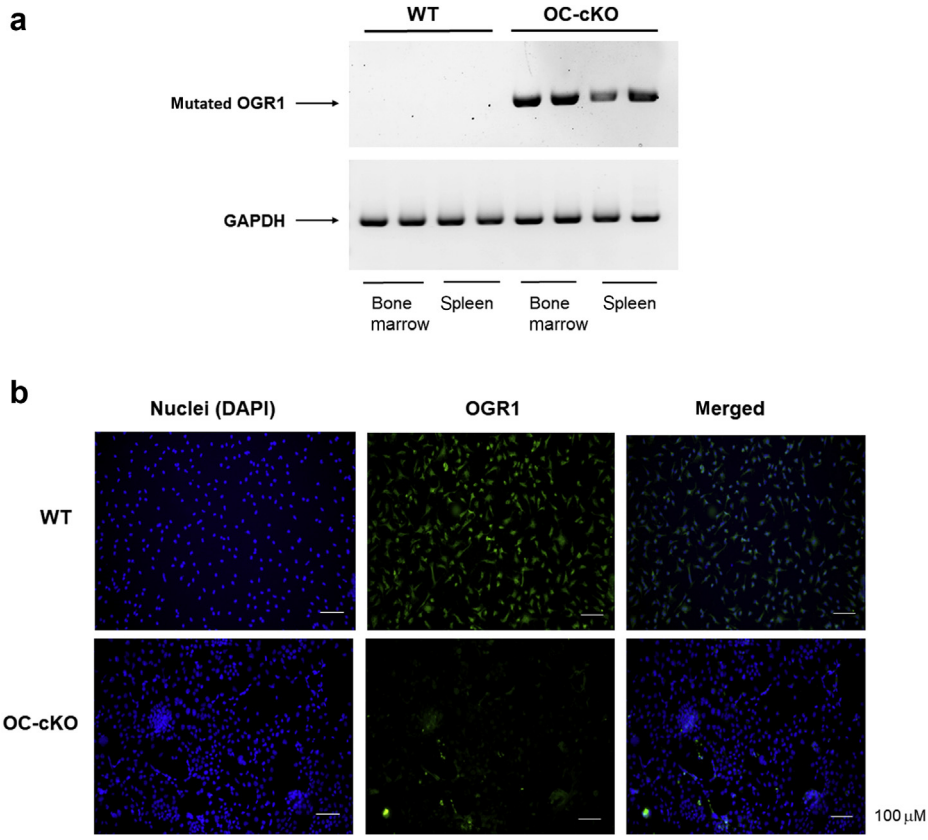

Figure 1 | Verification of *Ogr1* gene deletion and ovarian cancer G protein–coupled receptor 1 (OGR1)-specific immunostaining of differentiated osteoclasts (OCs) demonstrates an OC-specific deletion of OGR1 from OGR1 osteoclastic conditional knockout (OC-cKO) mice compared with wild-type (WT) mice. LysM-Cre and OGR1-floxed mice were bred and the offspring genotyped to obtain WT mice (OGR1-floxed mice, no cre) and mice that were homozygous for loss of intact OGR1 (OC-cKO, OC contain cre-recombinase, which has removed the OGR1 sequence flanked by loxP sites). (**a**) Bone marrow cells or spleen cells from 3-month-old female mice were differentiated to OCs as described in the Methods section, and these cells were used to verify the deletion of *Ogr1* alleles using a polymerase chain reaction primer specific for the mutated OGR1. Glyceraldehyde-3-phosphate dehydrogenase (*Gapdh*) was used as a housekeeping gene. (**b**) Bone marrow cells from 3-month-old female WT and OC-cKO mice were differentiated to OCs. Cells were fixed and stained with a specific primary antibody to OGR1 (green staining, center column). 4′,6-Diamidino-2-phenylindole (DAPI) staining (blue, left column) of nuclei demonstrates the presence of cells without OGR1 stain. Merged view of OGR1 and DAPI staining is shown in the right column. Original magnification ×20. Bar = 100 μM. To optimize viewing of this image, please see the online version of this article at www.kidney-international.org.

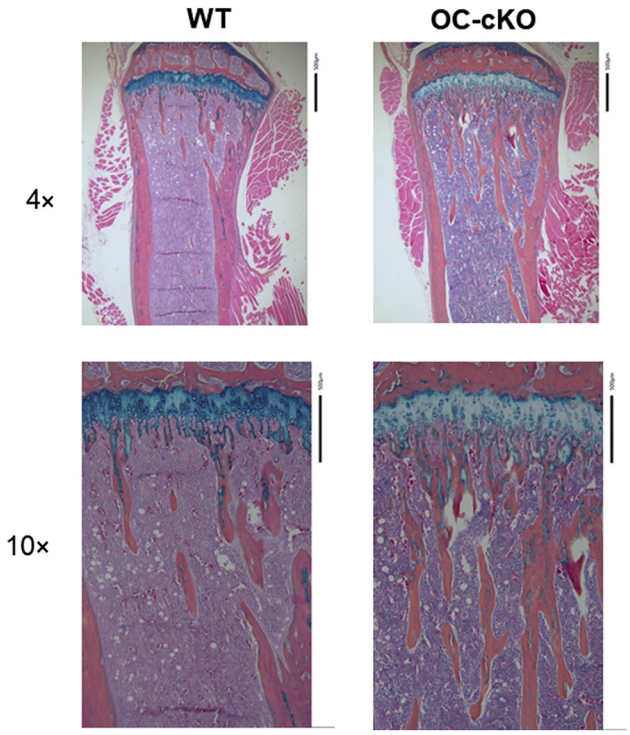

Figure 2 | Increased trabecular bone volume in the tibia metaphysis from 3-month-old female mouse with ovarian cancer G protein–coupled receptor 1 (OGR1) specifically deleted in osteoclasts. Bones were prepared for histochemical sectioning and stained with hematoxylin and eosin to show cellularity and Orange G to show bone. Left panels: Wild type (WT); right panels: osteoclastic conditional knockout (OC-cKO). Top panels: Original magnification ×4. Bottom panels: Original magnification ×10. Bar in each = 500 μM. To optimize viewing of this image, please see the online version of this article at www.kidney-international.org.

OGR1. Immunohistochemical staining of differentiated marrow cells also confirmed the successful deletion of intact OGR1 from OC in OC-cKO mice. Intact OGR1 is present in WT cells, but not in OC-cKO cells (Figure 1b).

Whole bone from OC-cKO and WT

Histochemical staining of the tibia metaphysis from 3-month-old female mice demonstrated increased trabecular bone volume in OC-cKO mice compared with WT mice (Figure 2). This is comparable to what we observed in global OGR1 knockout mice.[22] Micro-computed tomography (microCT) of both the femur (Figure 3a) and the tibia (Figure 3b) from OC-cKO mice also showed increased trabecular bone, as shown by increased bone volume/total volume and trabecular number in both the femur and the tibia and increased trabecular thickness and decreased trabecular separation in the tibia, as compared with WT mice. Increased cortical thickness and cortical area in OC-cKO mice were also found by microCT in both the femur and the tibia from 3-month-old female OC-cKO mice compared with WT mice (Table 1). MicroCT of vertebral trabecular and cortical bone from OC-cKO mice revealed no differences in these parameters compared with WT mice (Table 2). We have not found similar increases in bone density in male OC-cKO mice (Supplementary Figure S2).

Histology and microCT indicated increased bone density in OC-cKO mice compared to WT mice, suggesting less OC activity. We assessed OC activity by staining sections of tibiae from 3-month-old female mice with the specific OC stain tartrate-resistant acid phosphatase (TRAcP). We found decreased percent OC surface and OC number/bone surface in OC-cKO bone compared with WT bone (Figure 4).

Differentiated OCs from OC-cKO and WT cells

To characterize the resorption activity of isolated OCs, bone marrow cells (BMCs) were plated on bovine bone slices and differentiated to OCs *in vitro*. The resultant resorption pit formation was decreased with OC-cKO cells compared with WT cells (Figure 5). When BMCs were cultured *in vitro*, differentiated to OCs, and stained for TRAcP, cultures from OC-cKO cells also had a decreased number of OCs per well and those OCs were decreased in total area per well compared with cultures from WT OCs (Figure 6).

To further define the changes in OC activity, RNA expression of OC-specific genes was analyzed after BMCs were differentiated to OCs *in vitro*. Cathepsin K (*Ctsk*), matrix metalloproteinase 9 (*Mmp9*), TRAcP (*Tracp*), dendritic cell-specific transmembrane protein (*Dc-stamp*), nuclear factor of activated T cells 1 (*Nfatc1*), and receptor activator of nuclear factor kappaB (*Rank*) were all decreased in OCs from OC-cKO cells compared with WT cells (Figure 7).

OC-cKO and WT OC response to MET

To determine whether there were differences in the response of differentiated OCs to MET, we examined NFATc1 activation, which leads to its localization in the nucleus in OCs.[15,27] After initiating differentiation of BMCs in response to macrophage colony-stimulating factor (mCSF) for 2 days, medium was changed to preequilibrated physiological CO_2/HCO_3^- buffered neutral (pH 7.4) or MET (pH 7.1) medium and cells were incubated for an additional 45 minutes. Nuclear NFATc1 staining was increased with MET in WT cells; however, there was significantly less nuclear staining in OC-cKO cells (Figure 8). To further characterize the response of these OCs to MET, BMCs were differentiated to OCs with mCSF for 2 days, followed by the addition of RANKL for an additional 4 days. Cells were then switched to neutral or MET medium for 24 hours and stained with TRAcP. There was an increase in OC size and area in response to MET in WT cells; however, there was no change in OC size or area in OC-cKO cells (Figure 9).

DISCUSSION

In humans and mice, chronic MET induces increased cell-mediated bone resorption.[1,2,4] In mice, MET regulates osteoblast and osteoclast activity,[2,28] causing a decrease in both osteoblastic collagen synthesis and subsequent mineralization and an increase in osteoclastic bone resorption.[2] We have shown in cultured neonatal mouse calvariae that acid-induced

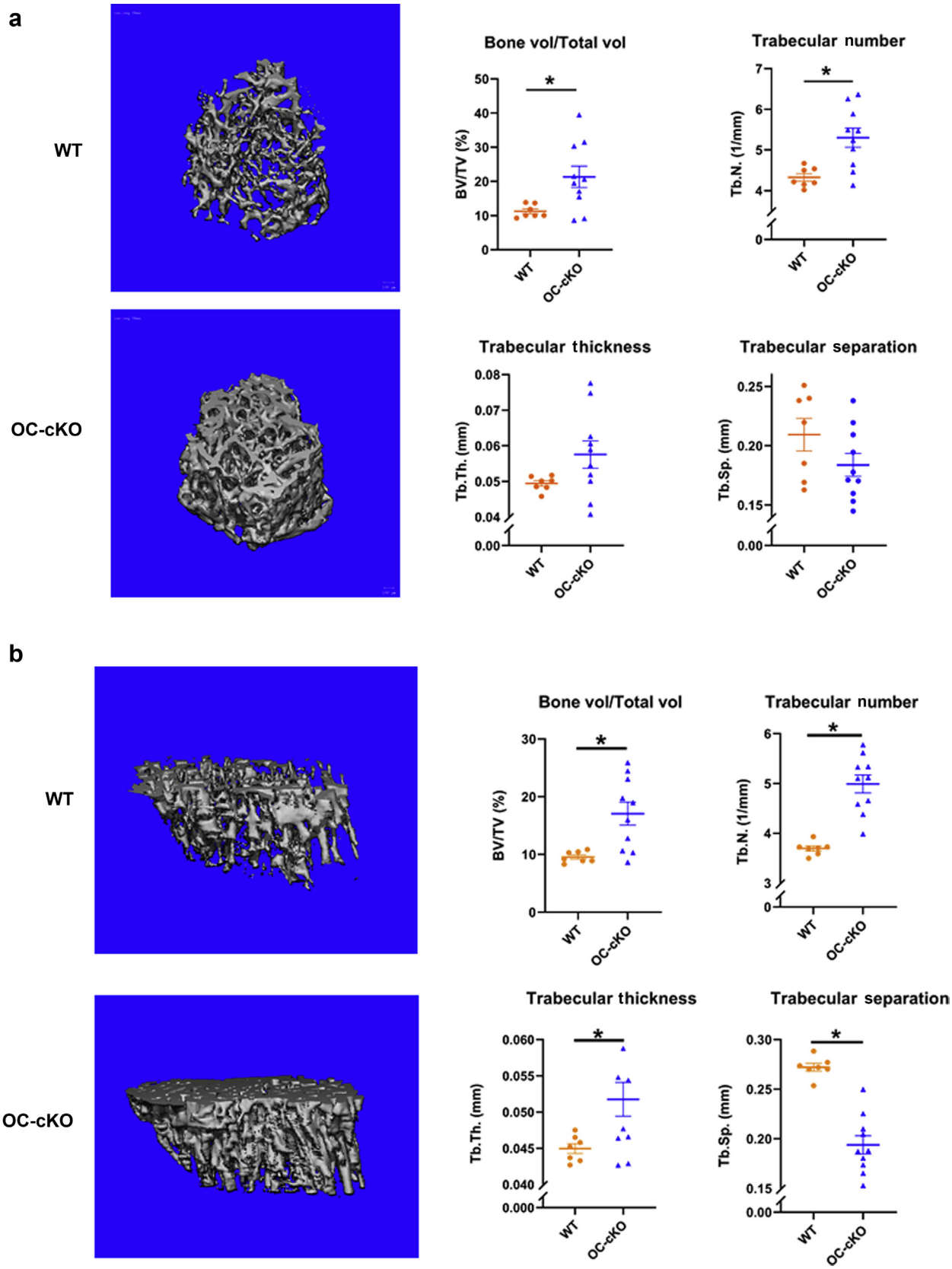

Figure 3 | Increased bone in the osteoclastic conditional knockout (OC-cKO) femur and tibia by micro-computed tomography (microCT) in 3-month-old female mouse trabecular bones compared with wild-type (WT) bones. Bones were prepared for microCT as described in the Methods section. (**a**) Representative femur trabecular bone (left panel) and quantitation of % bone volume/total (continued)

resorption is mediated through the G protein–coupled H^+ receptor OGR1.[7] Activation of OGR1 leads to inositol phosphate–mediated intracellular Ca signaling in osteoblasts.[7,20,21] We confirmed that OGR1 is present in primary mouse osteoblasts and that inhibition of OGR1 with $CuCl_2$ blocks MET-induced bone resorption in cultured calvariae.[7] Similarly, inhibition of inositol phosphate signaling in primary osteoblasts inhibited MET stimulation of cyclooxygenase 2 and RANKL, which are required to initiate MET-induced bone resorption in mouse calvariae.[9] A global deletion of OGR1 leads to increased BMD compared to WT mice,[22] presumably because of decreased acid-mediated bone resorption in response to the large endogenous acid production in rapidly growing mice.[29] We found an increase in osteoblastic gene expression, mineralization, and bone formation rate in these global knockout mice; however, histological analysis also demonstrated an increase in the number of OCs and their apparent activity, although OC activity was not measured directly.[22]

Our previous results in mouse osteoblasts suggested that OGR1 mediated the net resorptive response to MET.[7,22] Tomura *et al.* also found that OGR1 was the signal transducer for acid in human osteoblasts.[21] However, OGR1 is also present in OC.[24,26,30] It is not clear from our previous work whether MET-induced bone resorption was solely due to the regulation of osteoblast activity, through OGR1, which then mediated osteoclastic bone resorption or if OC OGR1 also directly contributed to MET-induced bone resorption. In the present study, we demonstrate that when OGR1 is specifically deleted from OCs, these OC-cKO mice exhibit increased BMD, which appears because of decreased OC activity in OC-cKO mice compared with WT mice. This is in contrast to what was observed histologically for OCs in global knockout mice. Both trabecular and cortical bone in long bones was increased, although, for reasons that are not clear from this study, there was no apparent change in vertebral bone. However, this may not be an unusual finding as Rowe *et al.*[31] reported that in a large number of individual gene knockouts, there was a differential effect on long bones and vertebral bones as well as dimorphism based on sex. Others have also found sex-related differences in phenotypes resulting from specific gene knockouts,[32–35] including a study of vitamin D receptor knockout that showed differences in skeletal phenotype.[36] Sexual dimorphism is present in many mammalian phenotypic traits,[37] and sex-chromosome dosage effects on gene expression have been found, though we do not yet know if that explains our results. Gene deletions themselves could also have effects not yet considered.

The decreased number and activity of OCs were also observed *in vitro* when marrow cells from these animals were differentiated to OCs. OC-specific gene expression was significantly decreased in differentiated OC-cKO cells compared with WT cells. The decreased gene expression was observed in multiple steps in the pathway for OC activation. RANK signaling activates NFATc1, a master regulator of OC differentiation and activity.[38] NFATc1 then induces dendritic cell-specific transmembrane protein, a transmembrane protein that plays a key role in OC fusion,[39,40] as well as inducing cathepsin K and TRAcP.[38] In addition to the decrease in baseline OC activity in OC-cKO mice, there was a decrease in the response of differentiated OC-cKO OCs to activation by physiological MET. This decreased response was observed for MET-induced NFATc1 nuclear accumulation as well as MET-induced increase in OC number and size.

In normal mice, MET induces a decrease in osteoblast bone formation and an increase in OC activity, leading to a marked increase in net bone resorption.[2,41] Our previous work indicates that the increased bone resorption by MET is mediated through the proton receptor OGR1.[22] We have shown that the loss of OGR1, either in both the osteoblast and the OC, as in global OGR1 knockout mice,[22] or just the OC, as in the present study of OC-cKO, leads to an increase in BMD. In global knockout mice, the large acid load of the rapidly growing mice appeared to increase osteoblast activity and also, on the basis of histology, increased OC activity compared with WT mice, though the increase in osteoblast activity must be greater than the observed increase in OC activity to account for the increase in BMD. However, in OC-cKO mice, although there was a similar increase in BMD, there was a decrease in OC activity consistent with the increase in BMD. Previously, we did not examine isolated OC from global OGR1 knockout mice, so we do not know whether the apparent increase in OC activity demonstrated only by bone histology was due to stimulation of the OC by the increase in osteoblast activity in the absence of OGR1. In OC-cKO mice, where the osteoblasts have normal OGR1

Table 1 | MicroCT of the 3-month-old female mouse femur and tibia demonstrates increased cortical bone in OC-cKO compared with WT bone

Bone	Thickness (mm)	Area (mm^2)
Femur		
WT	0.1983 ± 0.0038	0.8150 ± 0.0178
OC-cKO	0.2184 ± 0.0061[a]	1.0553 ± 0.0442[a]
Tibia		
WT	0.1859 ± 0.0033	0.7009 ± 0.0112
OC-cKO	0.2113 ± 0.0044[a]	0.9030 ± 0.0228[a]

MicroCT, micro-computed tomography; OC-cKO, osteoclastic conditional knockout; WT, wild type.
[a]$P < 0.05$ compared with WT.
Data are expressed as mean ± SEM for 10–11 bones per group.

Figure 3 | (continued) volume (BV/TV), trabecular number (Tb.N.), trabecular thickness (Tb.Th.), and trabecular separation (Tb.Sp.) (right panel). (**b**) Representative tibia trabecular bone (left panel) and quantitation of % BV/TV, Tb.N., Tb.Th., and Tb.Sp. (right panel). Data are expressed as mean ± SEM for 7 to 10 bones per group. *$P < 0.05$ compared with WT. To optimize viewing of this image, please see the online version of this article at www.kidney-international.org.

Table 2 | MicroCT of 3-month-old female mice demonstrates no change in vertebral trabecular or cortical bone in OC-cKO compared with WT bone

Trabecular bone	BV/TV (%)	Trabecular number	Trabecular thickness (mm)	Trabecular separation (mm)
WT	27.545 ± 0.665	5.424 ± 0.112	0.0519 ± 0.0008	0.1774 ± 0.0040
OC-cKO	28.432 ± 1.568	5.586 ± 0.111	0.0540 ± 0.0017	0.1666 ± 0.0045
Cortical bone	Cortical thickness (mm)	Cortical bone area (mm^2)		
WT	0.0785 ± 0.0011	1.2686 ± 0.0234		
OC-cKO	0.0725 ± 0.0007	1.2480 ± 0.0247		

BV/TV, bone volume/total volume; MicroCT, micro-computed tomography; OC-cKO, osteoclastic conditional knockout; WT, wild type.
Data are expressed as mean ± SEM for 10–11 bones per group.

activity, there would be no greater osteoblastic stimulation of OC activity by OC-cKO osteoblasts compared with WT mice, because in the presence of OGR1 in the osteoblast, MET would decrease OB bone formation as it does in normal (WT) mice. Clearly there is an important role of OGR1 in the OC and its direct response to MET in addition to our previously described role of OGR1 in the osteoblastic response to MET.[7,9,22] We have not studied osteocytes so that we cannot address any role that acidosis may have in altering function of this cell.

A role of OGR1 in the OC has also been demonstrated by others, although direct physiological responses to MET have not been characterized previously. Li *et al.* generated chimeric mice with germline OGR1 genes flanked by 2 loxP sites, which were bred to germline protamine-Cre mice to generate OGR1-deficient mice.[26] These mice, which had *Ogr1* genes deleted at a very early stage, exhibited decreased melanoma tumorigenesis and increased proliferation of brown adipose tissue. The bones of these mice showed no gross abnormalities, but isolated differentiated OC from these mice showed decreased osteoclastogenesis and a resistance to a pH-dependent decrease in survival, though the pH changes used nonphysiological buffers and a nonphysiological pH of ≤6.8. The authors suggested that OGR1's role in

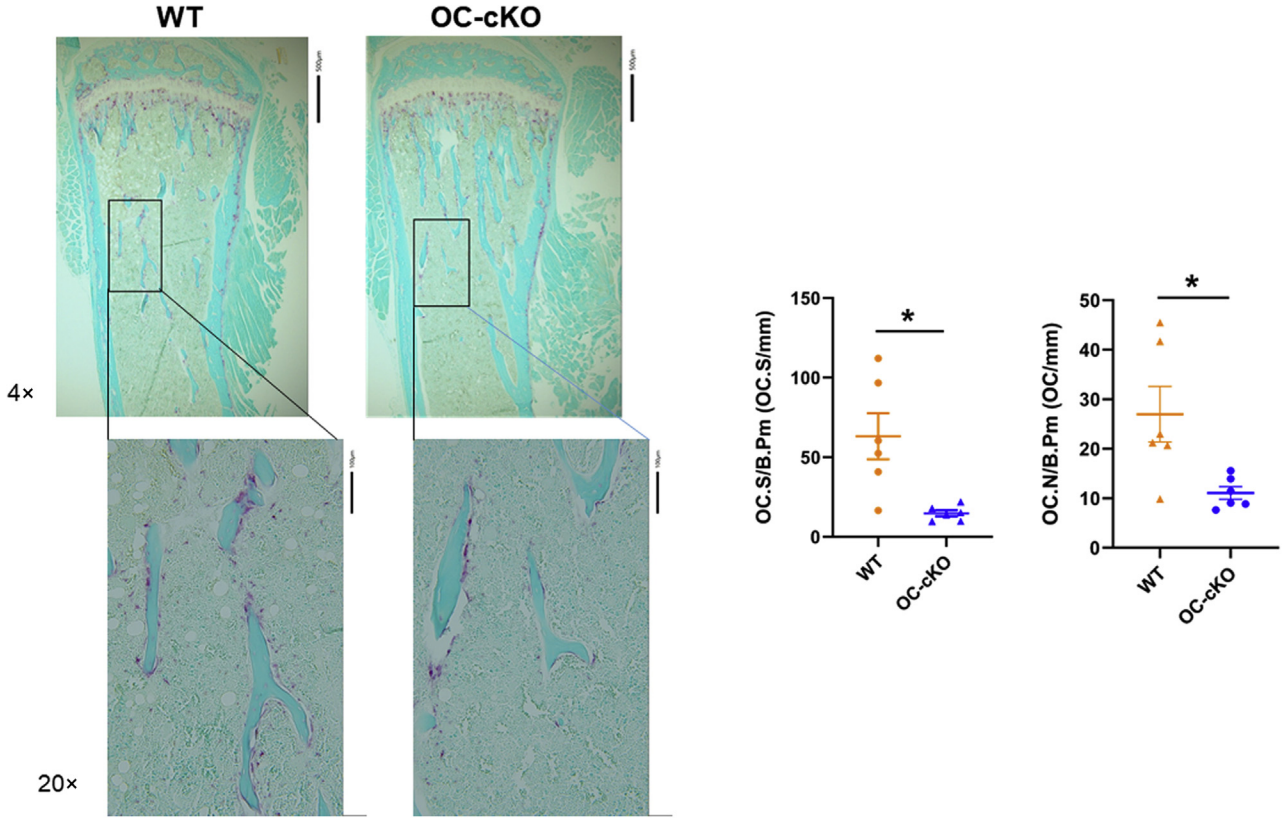

Figure 4 | Decreased tartrate-resistant acid phosphatase (TRAcP) staining of osteoclasts (OCs) in tibiae from 3-month-old female mice with an OC-specific deletion of ovarian cancer G protein–coupled receptor 1 compared with wild-type (WT) mice. Left panel: Representative histochemical staining for TRAcP in WT and osteoclastic conditional knockout (OC-cKO) tibiae. Upper images: Original magnification ×4; bar = 500 μM. Lower images: Original magnification ×20; bar = 100 μM. Right panel: Quantitation of OC surface/bone surface (OC.S/b.Pm) and OC number/bone surface (OC.N/B.Pm) according to TRAcP staining. Data are expressed as mean ± SEM for 6 bone sections per group. *$P < 0.05$ compared with WT. To optimize viewing of this image, please see the online version of this article at www.kidney-international.org.

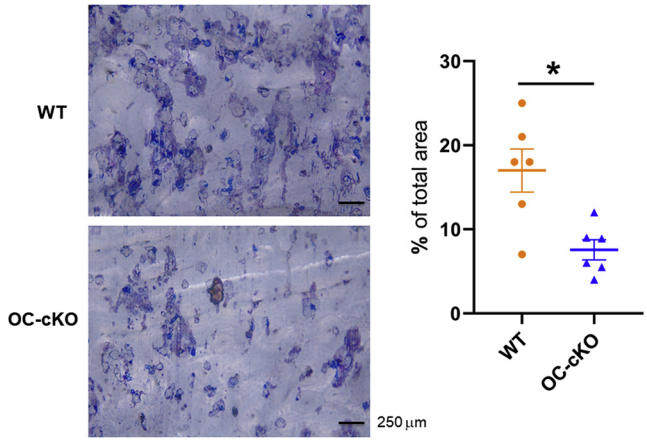

Figure 5 | Decreased resorption pit formation by differentiated osteoclasts cultured from marrow stromal cells from osteoclastic conditional knockout (OC-cKO) mice compared with wild-type (WT) mice. Bone marrow cells from WT and OC-cKO mice were plated on bovine slices and induced to differentiate in the presence of macrophage colony-stimulating factor and receptor activator of nuclear factor κB ligand. After 13 days, cells were removed from the bone slices and pit formation was visualized with toluidine blue and pit area quantified. Left panels: Representative images of bone slices. Bar in each = 250 μM. Right panel: Quantitation of pit area as % total area scanned. Data are expressed as mean ± SEM of 6 samples. *$P < 0.05$ compared with WT. To optimize viewing of this image, please see the online version of this article at www.kidney-international.org.

osteoclastogenesis was not strong enough to affect overall bone development. We used this OGR1 fl/fl mouse to generate our OC-specific knockout mice to directly address the role of OGR1 in response to MET by using only the physiological CO_2/HCO_3^- buffer system within the physiological pH range of 7.40 to 7.10.[42] Komarova *et al.* demonstrated an increased intracellular Ca-mediated nuclear accumulation of NFATc1 in rat and rabbit OCs in an acid environment, although, again, nonphysiological buffers were used to compare responses at pH 7.6 to 7.0.[23] A transient increase in intracellular Ca was observed when pH was lowered to 7.0, which was inhibited by Zn, a known inhibitor of OGR1. *Ogr1* mRNA also increased with differentiation of RAW 264.7 cells, which suggested these responses occur via activation of OGR1. Yang *et al.* found that OGR1 was upregulated after the treatment of CSF-null osteopetrotic rats with mCSF *in vivo*.[24] This upregulation was also observed *in vitro* in mouse bone marrow cells and RAW 264.7 preosteoclastic cells after CSF-1– and RANKL-induced OC differentiation, suggesting that OGR1 is expressed early during osteoclastogenesis and is important in OC differentiation. Iwai *et al.* showed that regulator of G-protein signaling 18, which is inhibited after activation of the RANKL/RANK system, is a negative regulator of osteoclastogenesis that acts through the OGR1/NFAT pathway.[25] In contrast to the results of Li *et al.*,[26] Pereverzev *et al.* showed that OC survival was enhanced by acidification of disaggregated rat OCs and RAW 264.7 cells, though, again, nonphysiological buffers were used to adjust the pH to 7.6 or 7.0.[30] This effect was independent of NFAT activation. A role for OGR1 was suggested by increased Ca signaling in medium at pH 6.4 that was inhibited by Cu^{2+} or RNA interference directed at OGR1, though this pH is far below the physiological limit of mammalian survival.[42] Most recently, Imenez Silva *et al.* studied a global OGR1 knockout mouse model, but found no change in BMD or OC activity.[19] Direct comparisons of this global OGR1 knockout with our OC-specific knockout are not possible as development of the models was different and they did not report any bone histochemical or microCT analyses.

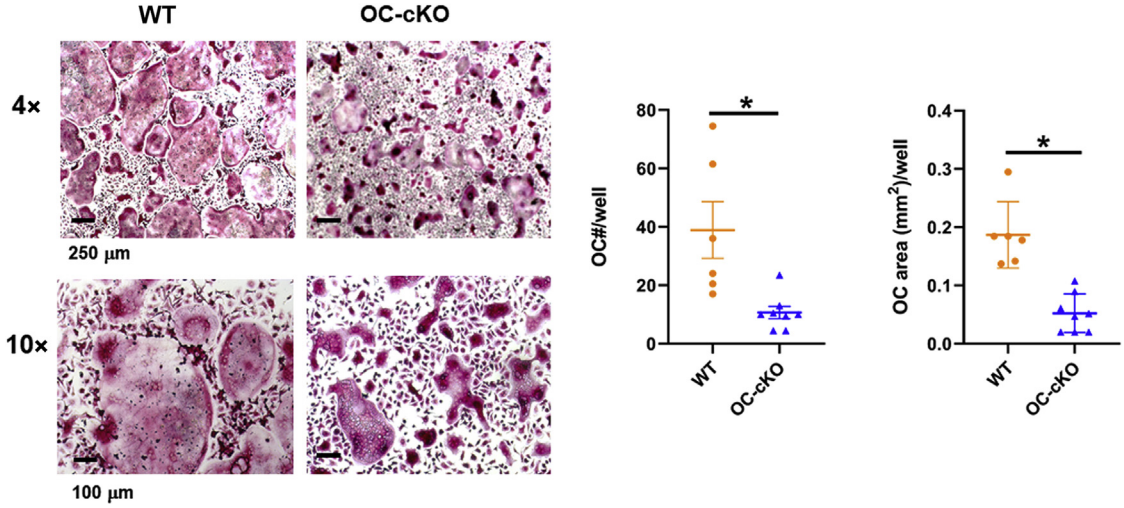

Figure 6 | Decreased tartrate-resistant acid phosphatase (TRAcP) staining of differentiated osteoclasts cultured from marrow stromal cells from osteoclastic conditional knockout (OC-cKO) mice compared with wild-type (WT) mice. Left panel: Representative histochemical staining for TRAcP in cells differentiated in the presence of macrophage colony-stimulating factor and receptor activator of nuclear factor κB ligand as described in the Methods section. Upper images: Original magnification ×4; bar in each = 250 μM. Lower images: Original magnification ×10; bar in each = 100 μM. Right panel: Quantitation of OC number per well and OC area per well. Data are mean ± SEM for 6–7 cultures per group. *$P < 0.05$ compared to WT. To optimize viewing of this image, please see the online version of this article at www.kidney-international.org.

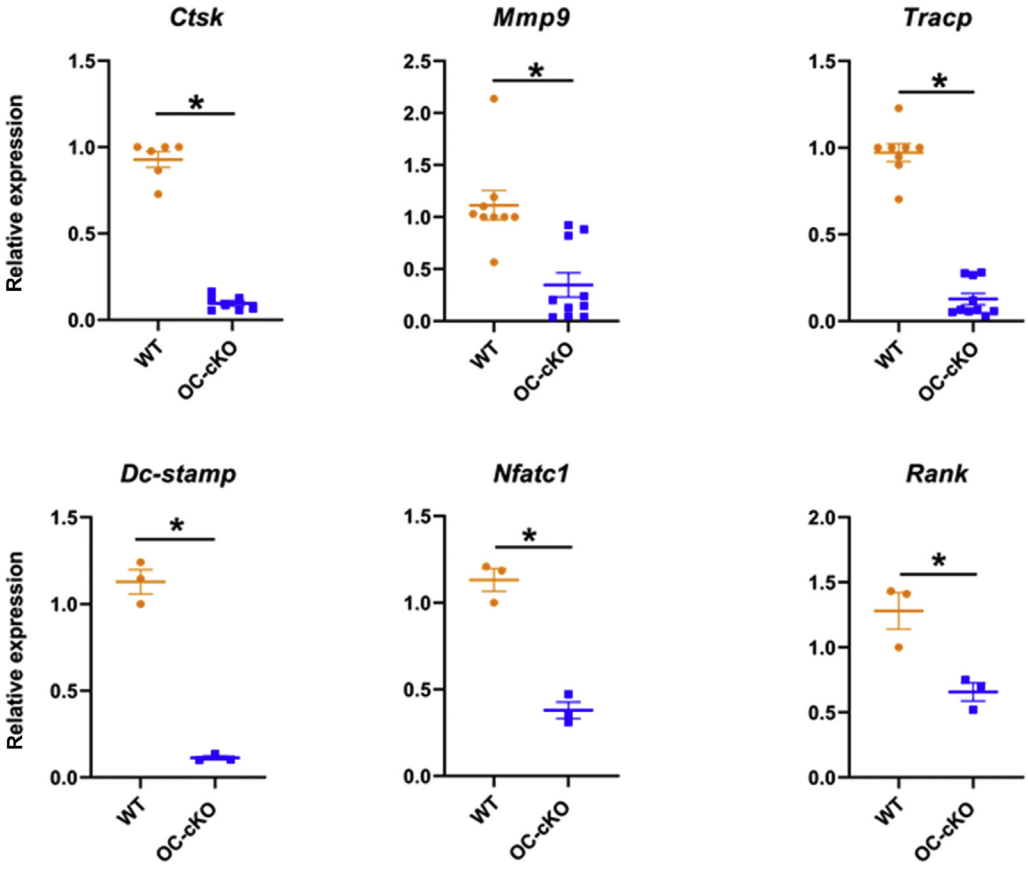

Figure 7 | Decreased osteoclastic RNA expression in differentiated marrow stromal cells (MSCs) from osteoclastic conditional knockout (OC-cKO) marrow compared with wild-type (WT) mice. MSCs from WT and OC-cKO mice were differentiated in culture in the presence of macrophage colony-stimulating factor and receptor activator of nuclear factor κB ligand (RANKL) as described in the Methods section. Total RNA was isolated and relative expression of cathepsin K (*Ctsk*), matrix metalloproteinase 9 (*Mmp9*), tartrate-resistant acid phosphatase (*Tracp*), dendritic cell-specific transmembrane protein (*Dc-stamp*), nuclear factor of activated T cells 1 (*Nfatc1*), and receptor activator of nuclear factor kappaB (*Rank*) were analyzed by quantitative polymerase chain reaction relative to the housekeeping gene *Rpl13a*. Data are expressed as mean ± SEM for 5 to 10 replicate cultures per group. *$P < 0.05$ compared with WT.

MET induces bone loss due to a negative bone balance by directly decreasing osteoblastic bone formation and increasing osteoclastic bone resorption. Before this study, we did not know whether the effects of MET on the OC were mediated solely through the osteoblast or included a component of direct action on the OC. Using cultured OCs from an OC-specific knockout of OGR1 and a physiological CO_2/HCO_3^- buffer system to simulate clinical MET, we now demonstrate that acidosis can directly stimulate OC OGR1 to increase osteoclastic bone resorption in addition to its regulation of osteoblast activity.

Patients with chronic kidney disease and those on dialysis have significant abnormalities in bone quality, leading to an increased incidence of fractures.[43,44] During chronic kidney disease, net acid excretion falls below endogenous acid production, leading to acid retention and the clinical disorder of MET. We and others have shown that MET adversely affects bone, leading to enhanced cell-mediated bone resorption and decreased bone formation. OGR1 is the proton receptor that senses the acid/base environment of bone. Characterization of the role of OGR1 in MET-induced bone resorption may help in understanding bone loss in these patients with acidosis and chronic kidney disease and may lead to the development of specific treatment.

METHODS

Generation of OC-specific knockout mouse

We obtained OGR1 fl/fl mice from Dr. Yan Xu, Indiana University School of Medicine.[26] To generate OC-specific OGR1 conditional knockout mouse, OGR1 fl/fl mice were bred with LysM-Cre transgenic mice. To identify mice containing flox and cre alleles, genotyping was performed by PCR using genomic DNA from tail snips. OGR1 fl/fl mice are defined as WT. All experiments were performed in accordance with the National Institutes of Health guidelines and approved by the University of Rochester Medical Center Animal Care Committee.

MicroCT

To assess bone microstructure, the right femur, tibiae, and L2 vertebrate were isolated from OC-cKO and age-matched WT female mice after killing using CO_2 inhalation. Bones were fixed in 10% neutral buffered formalin for scanning using a vivaCT 40 microCT scanner (Scanco Medical, Bruttisellen, Switzerland). Three-dimensional

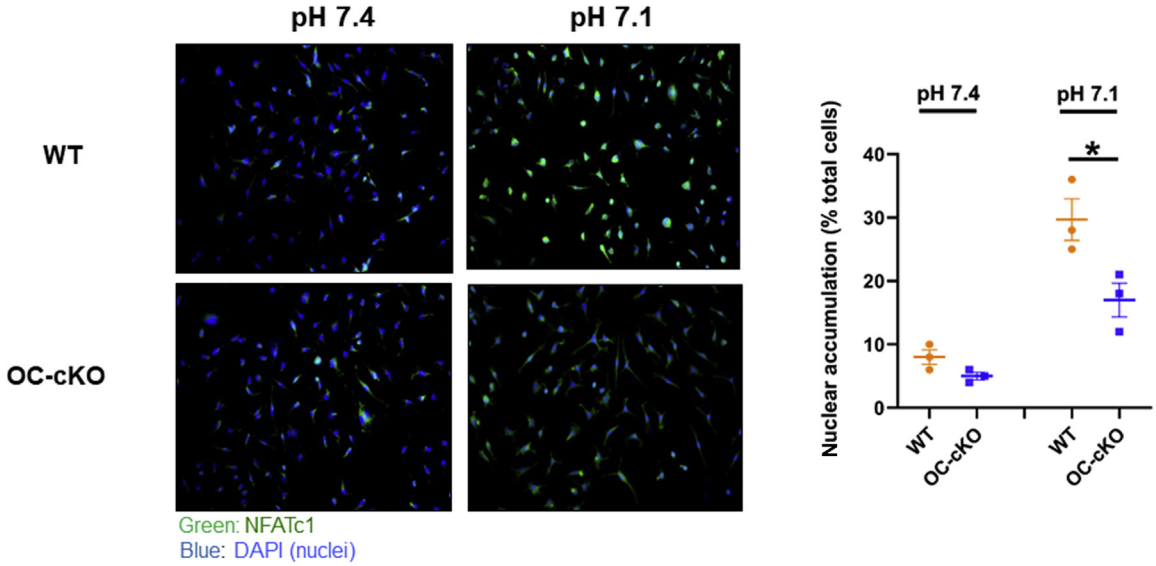

Figure 8 | Decreased acid-dependent translocation of nuclear factor of activated T cells 1 (NFATc1) from the cytoplasm to nuclei by immunofluorescent staining in cells derived from marrow stromal cells from osteoclastic conditional knockout (OC-cKO) mice compared with wild-type (WT) mice. MSCs from WT and OC-cKO mice were incubated with macrophage colony-stimulating factor for 3 days, and then culture medium was changed to preequilibrated physiological CO_2/HCO_3^- buffered neutral (pH 7.4) or acid (pH 7.1) medium for an additional 45 minutes. Cells were then fixed as described in the Methods section, and immunofluorescent staining for NFATc1 in nuclei was assessed. Left panel: Representative fluorescent staining at pH 7.4 and 7.1. Right panel: Quantitation of nuclear accumulation of fluorescence as a function of total number of cells at pH 7.4 and 7.1. Data are expressed as mean ± SEM for 3 cultures per group. *$P < 0.05$ compared with WT at the same pH. DAPI, 4′,6-diamidino-2-phenylindole. To optimize viewing of this image, please see the online version of this article at www.kidney-international.org.

reconstructions generated from 2-dimensional images were used to calculate morphometric parameters.

Histomorphometric analysis of bone sections

Tibiae were removed from 3-month-old female WT and OC-cKO mice after killing as described above. Cleaned tibiae were fixed, decalcified, and embedded in paraffin. Sections (5 μm) were stained with hematoxylin and eosin and Orange G and for TRAcP activity at the University of Rochester Orthopedic Core facility. Histomorphometric analysis of OC numbers and surface, expressed per millimeter bone surface, were performed using Osteometrics image analysis software (Osteometrics, Inc., Decatur, GA).

OC cultures from BMCs

Bone marrow hematopoietic stem cells (BMCs) were isolated from femurs of 10- to 12-week-old female WT and OC-cKO mice.[45] To

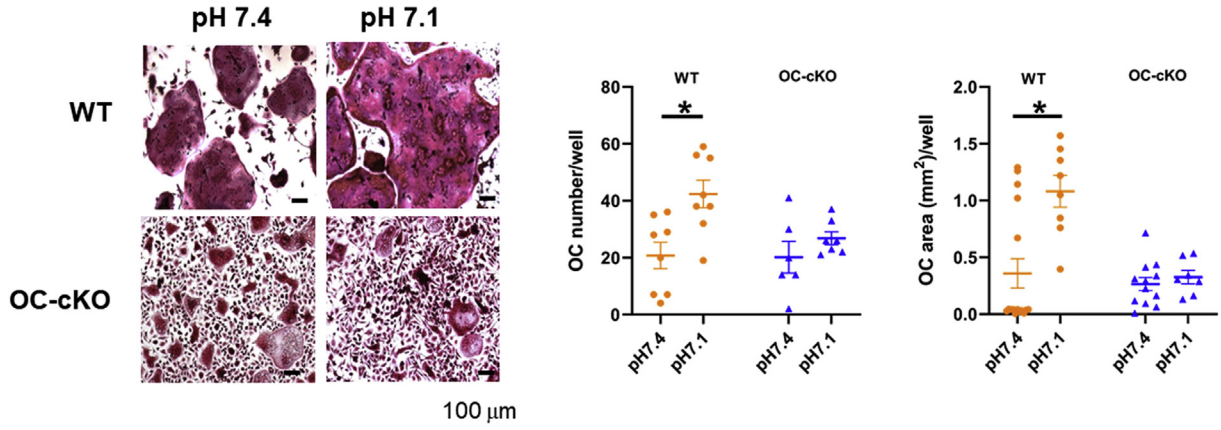

Figure 9 | Decreased acid response of differentiated osteoclasts (OCs) from osteoclastic conditional knockout (OC-cKO) marrow stromal cells (MSCs) compared with OCs from wild-type (WT) mice. MSCs from WT and OC-cKO mice were differentiated in culture in the presence of macrophage colony-stimulating factor and receptor activator of nuclear factor κB ligand as described in the Methods section. After differentiation, culture medium was changed to preequilibrated physiological CO_2/HCO_3^- buffered neutral (pH 7.4) or acid (pH 7.1) medium for an additional 24 hours. Left panel: Representative tartrate-resistant acid phosphatase staining of OCs after differentiation of MSCs and subsequent incubation at pH 7.4 or 7.1 medium. Original magnification ×10. Bar in each = 100 μM. Right panel: Quantitation of OC number per well and OC area per well. Data are expressed as mean ± SEM for 6 to 12 replicate cultures per group. *$P < 0.05$ compared with pH 7.4 for OCs from WT mice. To optimize viewing of this image, please see the online version of this article at www.kidney-international.org.

generate OCs, BMCs were cultured in α-Eagle minimal essential medium (Corning, Ref 15-012-CV) containing 5 ng/ml of mCSF. After 2 days, fresh medium also containing 25 ng/ml of RANKL was added and cells were cultured for an additional 4 days to induce OC differentiation. Cells in 96-well plates were then stained for TRAcP. Dark red TRAcP-positive cells having ≥3 nuclei were counted as OCs. Total RNA was isolated from 100-mm plates and used for quantitative PCR analysis of specific osteoclastic gene expression. In indicated experiments, medium was changed to preequilibrated neutral (pH 7.4) or acid medium (pH 7.1) containing mCSF and RANKL for an additional 20 to 24 hours. Medium pH was adjusted by the addition of 2.4 N HCl to reduce bicarbonate concentration as a physiological model of MET, and the partial pressure of CO_2 was maintained at the physiological normal of ∼40 mm Hg.[4,17,46]

OC cultures from spleens

To generate OCs from spleens of WT and OC-cKO mice, 3-month-old female mice were killed as described above. Spleens were removed and cells disaggregated[47] and plated in α-Eagle minimal essential medium containing 10% heat-inactivated fetal bovine serum and 1% L-glutamine plus mCSF (5 ng/ml). After 2 days of incubation, fresh medium containing RANKL (25 ng/ml) was added to the cells and cultures continued up to 7 days. Cells were then harvested for PCR.

Resorption pit formation

BMCs were isolated from femurs of 3-month-old female WT and OC-cKO mice as described above. Cells were cultured on one 50-μm-thick bovine cortical bone slice per well in a 96-well plate and incubated with α-Eagle minimal essential medium containing mCSF (5 ng/ml).[48] After 2 days, medium was changed to fresh medium also containing RANKL (25 ng/ml) and cells were cultured for 12 days. The bone slices were removed from the wells, fixed, and washed, and resorption pit formation was visualized with toluidine blue and quantified using ImageJ (National Institutes of Health, Bethesda, MD, version 1.50i).

Immunofluorescence

Immunofluorescent staining of cells grown on coverslips was performed according to the protocol of Poligone *et al.*[49] Cells were fixed, washed, and then permeabilized. After blocking, cells were stained with primary antibody to OGR1 followed by the secondary antibody and nuclei were counterstained with the fluorescent dye 4′,6-diamidino-2-phenylindole.

Real-time quantitative PCR

Total RNA was extracted using an RNeasy Mini Kit (Qiagen, Hilden, Germany) and used for cDNA synthesis. Quantitative real-time PCR was performed using SYBR Green Supermix (BioRad, Hercules, CA). Quantification of PCR products was done using the comparative cycle threshold method as described previously.[50] *Rpl13a* was used as an internal control to determine the relative expression of each gene.

NFATc1 nuclear accumulation

Bone marrow cells were isolated from femurs of 3-month-old female WT and OC-cKO mice as described above. To assess the effect of MET on the nuclear accumulation of NFATc1 in OCs, BMCs were seeded on glass coverslips in a 6-well plate in α-Eagle minimal essential medium containing mCSF (5 ng/ml). After 3 days, medium was replaced with preequilibrated neutral medium (pH 7.4) or MET medium (pH 7.1) for 45 minutes. Medium pH was adjusted with 2.4 N HCl as described above. After incubation, cells were fixed, permeabilized, and then stained with a primary antibody to NFATc1 followed by a secondary antibody and counterstained with 4′,6-diamidino-2-phenylindole for nuclei identification.

Data analysis

Statistical analysis was performed using the Student *t* test for unpaired comparisons. Data are presented as mean ± SEM, and $P < 0.05$ was considered significant.

SUPPLEMENTAL MATERIAL

Supplementary File (PDF)

Supplementary Detailed Methods.

Figure S1. Osteoclast specific deletion of OGR1.

Figure S2. No difference in OC-cKO tibia by microCT in 3-month-old male mouse trabecular bone compared to wild-type bones.

DISCLOSURE

NSK reports grants from the Renal Research Institute and the National Institutes of Health (NIH) to support this research. She owns stocks and stock options from Tricida and stocks from Amgen. Her spouse is a consultant for Tricida, Sanofi Genzyme, and Relypsa/Vifor Fresenius; receives speaking fees from Sanofi Genzyme; and is an adjudicator for adverse events from Novo Nordisk/Covance (outside the submitted work). DAB reports a grant from the NIH and personal fees and other from Tricida, Amgen, Relypsa/Vifor Fresenius, and Sanofi Genzyme (outside the submitted work). All the other authors declared no competing interests.

ACKNOWLEDGMENTS

This work was supported by grant RO1 DK075462 from the National Institutes of Health to DAB and a grant from the Renal Research Institute to NSK.

REFERENCES

1. Lemann J Jr, Bushinsky DA, Hamm LL. Bone buffering of acid and base in humans. *Am J Physiol Renal Physiol*. 2003;285:F811–F832.
2. Krieger NS, Sessler NE, Bushinsky DA. Acidosis inhibits osteoblastic and stimulates osteoclastic activity in vitro. *Am J Physiol*. 1992;262:F442–F448.
3. Bushinsky DA, Wolbach W, Sessler NE, et al. Physicochemical effects of acidosis on bone calcium flux and surface ion composition. *J Bone Miner Res*. 1993;8:93–102.
4. Bushinsky DA, Goldring JM, Coe FL. Cellular contribution to pH-mediated calcium flux in neonatal mouse calvariae. *Am J Physiol*. 1985;248:F785–F789.
5. Bushinsky DA, Krieger NS, Geisser DI, et al. Effects of pH on bone calcium and proton fluxes in vitro. *Am J Physiol*. 1983;245:F204–F209.
6. Bushinsky DA. Net calcium efflux from live bone during chronic metabolic, but not respiratory, acidosis. *Am J Physiol*. 1989;256:F836–F842.
7. Frick KK, Krieger NS, Nehrke K, et al. Metabolic acidosis increases intracellular calcium in bone cells through activation of the proton receptor OGR1. *J Bone Miner Res*. 2009;24:305–313.
8. Ori Y, Lee SG, Krieger NS, et al. Osteoblastic intracellular pH and calcium in metabolic and respiratory acidosis. *Kidney Int*. 1995;47:1790–1796.
9. Krieger NS, Bushinsky DA. Pharmacologic inhibition of intracellular calcium release blocks acid-induced bone resorption. *Am J Physiol Renal Physiol*. 2011;300:F91–F97.
10. Krieger NS, Frick KK, LaPlante Strutz K, et al. Regulation of COX-2 mediates acid-induced bone calcium efflux in vitro. *J Bone Miner Res*. 2007;22:907–917.
11. Frick KK, Krieger NS, LaPlante K, et al. Decreased acid-induced bone resorption in COX-2 knockout mice. *J Bone Miner Res*. 2004;19(suppl 1):5188.
12. Frick KK, Bushinsky DA. Metabolic acidosis stimulates RANK ligand RNA expression in bone through a cyclooxygenase dependent mechanism. *J Bone Miner Res*. 2003;18:1317–1325.

13. Frick KK, LaPlante K, Bushinsky DA. RANK ligand and TNF-alpha mediate acid-induced bone calcium efflux in vitro. *Am J Physiol Renal Physiol*. 2005;289:F1005–F1011.
14. Martin TJ, Sims NA. RANKL/OPG; critical role in bone physiology. *Rev Endocr Metab Disord*. 2015;16:131–139.
15. Boyce BF. Advances in osteoclast biology reveal potential new drug targets and new roles for osteoclasts. *J Bone Miner Res*. 2013;28:711–722.
16. Krieger NS, Culbertson CD, Kyker-Snowman K, et al. Metabolic acidosis increases fibroblast growth factor 23 in neonatal mouse bone. *Am J Physiol Renal Physiol*. 2012;303:F431–F436.
17. Krieger NS, Bushinsky DA. Stimulation of fibroblast growth factor 23 by metabolic acidosis requires osteoblastic intracellular calcium signaling and prostaglandin synthesis. *Am J Physiol Renal Physiol*. 2017;313:F882–F886.
18. Wiley SZ, Sriram K, Salmerón C, et al. GPR68: an emerging drug target in cancer. *Int J Mol Sci*. 2019;20:559.
19. Imenez Silva PH, Katamesh-Benabbas C, Chan K, et al. The proton-activated ovarian cancer G protein-coupled receptor 1 (OGR1) is responsible for renal calcium loss during acidosis. *Kidney Int*. 2020;97:920–933.
20. Ludwig MG, Vanek M, Gueirine D, et al. Proton-sensing G-protein-coupled receptors. *Nature*. 2003;425:93–98.
21. Tomura H, Wang JQ, Liu Jp, et al. Cyclooxygenase-2 expression and prostaglandin E2 production in response to acidic pH through OGR1 in a human osteoblastic cell line. *J Bone Miner Res*. 2008;23:1129–1139.
22. Krieger NS, Yao Z, Kyker-Snowman K, et al. Increased bone density in mice lacking the proton receptor OGR1. *Kidney Int*. 2016;89:565–573.
23. Komarova SV, Pereverzev A, Shum JW, et al. Convergent signaling by acidosis and receptor activator of NF-kB ligand (RANKL) on the calcium/calcineurin/NFAT pathway in osteoclasts. *Proc Natl Acad Sci U S A*. 2005;102:2643–2648.
24. Yang M, Mailhot G, Birnbaum MJ, et al. Expression of and role for ovarian cancer G-protein-coupled receptor 1 (OGR1) during osteoclastogenesis. *J Biol Chem*. 2006;281:23598–23605.
25. Iwai K, Koike M, Ohshima S, et al. RGS18 acts as a negative regulator of osteoclastogenesis by modulating the acid-sensing OGR1/NFAT signaling pathway. *J Bone Miner Res*. 2007;22:1612–1620.
26. Li H, Wang D, Singh LS, et al. Abnormalities in osteoclastogenesis and decreased tumorigenesis in mice deficient for ovarian cancer G protein-coupled receptor 1. *PLoS One*. 2009;4:e5705.
27. Zhao Q, Wang X, Liu Y, et al. NFATc1: functions in osteoclasts. *Int J Biochem Cell Biol*. 2010;42:576–579.
28. Krieger NS, Frick KK, Bushinsky DA. Mechanism of acid-induced bone resorption. *Curr Opin Nephrol Hypertens*. 2004;13:423–436.
29. Singer D. Metabolic adaptation to hypoxia: cost and benefit of being small. *Respir Physiol Neurobiol*. 2004;141:215–228.
30. Pereverzev A, Komarova SV, Korcok J, et al. Extracellular acidification enhances osteoclast survival through an NFAT-independent, protein kinase C-dependent pathway. *Bone*. 2008;42:150–161.
31. Rowe DW, Adams DJ, Hong S-H, et al. Screening gene knockout mice for variation in bone mass: analysis by μCT and histomorphometry. *Curr Osteoporos Rep*. 2018;16:77–94.
32. Chella Krishnan K, Sabir S, Shum M, et al. Sex-specific metabolic functions of adipose lipocalin-2. *Mol Metab*. 2019;30:30–47.
33. Caetano MS, Hassane M, Van HT, et al. Sex specific function of epithelial STAT3 signaling in pathogenesis of K-ras mutant lung cancer. *Nat Commun*. 2018;9:4589.
34. Young JA, Jensen EA, Stevens A, et al. Characterization of an intestine-specific GH receptor knockout (IntGHRKO) mouse. *Growth Horm IGF Res*. 2019;46–47:5–15.
35. Vomhof-DeKrey EE, Lee J, Lansing J, et al. Schlafen 3 knockout mice display gender-specific differences in weight gain, food efficiency, and expression of markers of intestinal epithelial differentiation, metabolism, and immune cell function. *PLoS One*. 2019;14:e0219267.
36. Ryan JW, Starczak Y, Tsangari H, et al. Sex-related differences in the skeletal phenotype of aged vitamin D receptor global knockout mice. *J Steroid Biochem Mol Biol*. 2016;164:361–368.
37. Karp NA, Mason J, Beaudet AL, et al. Prevalence of sexual dimorphism in mammalian phenotypic traits. *Nat Commun*. 2017;8:15475.
38. Park JH, Lee NK, Lee SY. Current understanding of RANK signaling in osteoclast differentiation and maturation. *Mol Cells*. 2017;40:706–713.
39. Yagi M, Miyamoto T, Toyama Y, et al. Role of DC-STAMP in cellular fusion of osteoclasts and macrophage giant cells. *J Bone Miner Metab*. 2006;24:355–358.
40. Zhang C, Dou C, Xu J, et al. DC-STAMP, the key fusion-mediating molecule in osteoclastogenesis. *J Cell Physiol*. 2014;229:1330–1335.
41. Bushinsky DA, Chabala JM, Gavrilov KL, et al. Effects of in vivo metabolic acidosis on midcortical bone ion composition. *Am J Physiol*. 1999;277:F813–F819.
42. Palmer BF. Normal acid-base balance. In: Johnson RJ, Feehally J, Floege J, eds. *Comprehensive Clinical Nephrology*. 5th ed. Philadelphia, PA: Elsevier; 2015:142–148.
43. Jadoul M, Albert JM, Akiba T, et al. Incidence and risk factors for hip or other bone fractures among hemodialysis patients in the Dialysis Outcomes and Practice Patterns Study. *Kidney Int*. 2006;70:1358–1366.
44. Nickolas TL, Leonard MB, Shane E. Chronic kidney disease and bone fracture: a growing concern. *Kidney Int*. 2008;74:721–731.
45. Xiu Y, Xu H, Zhao C, et al. Chloroquine reduces osteoclastogenesis in murine osteoporosis by preventing TRAF3 degradation. *J Clin Investig*. 2014;124:297–310.
46. Bushinsky DA. Stimulated osteoclastic and suppressed osteoblastic activity in metabolic but not respiratory acidosis. *Am J Physiol*. 1995;268:C80–C88.
47. Boraschi-Diaz I, Komarova SV. The protocol for the isolation and cryopreservation of osteoclast precursors from mouse bone marrow and spleen. *Cytotechnology*. 2016;68:105–114.
48. Bradley EW, Oursler MJ. Osteoclast culture and resorption assays. In: Westendorf JJ, ed. *Osteoporosis: Methods and Protocols*. Totowa, NJ: Humana Press; 2008:19–35.
49. Poligone B, Gilmore ES, Alexander CV, et al. PKK suppresses tumor growth and is decreased in squamous cell carcinoma of the skin. *J Invest Dermatol*. 2015;135:869–876.
50. Livak KJ, Schmittgen TD. Analysis of relative gene expression data using real-time quantitative PCR and the 2-(Delta Delta C(T)) method. *Methods*. 2001;25:402–408.